Supporting Information

Manufacturing Macroporous Monoliths of Microporous Metal Organic Frameworks (MOFs)

Remo N. Widmer[§]*, Giulio. I. Lampronti*[§]*, Benjamin Kunz*[†]*, Corsin Battaglia*[†]*, Jennifer H. Shepherd*[‡]*, Simon A. T. Redfern*[§]**, Thomas D. Bennett*[‡]

§ Department of Earth Sciences, University of Cambridge, Downing Street, Cambridge, CB2 3EQ, United Kingdom

† Empa, Swiss Federal Laboratories for Materials Science and Technology, Ueberlandstrasse 129, CH-8600 Duebendorf, Switzerland

‡ Department of Materials Sciences & Metallurgy, 27 Charles Babbage Road, Cambridge, CB30FS, United Kingdom

* E-mail: satr@cam.ac.uk

Synthesis, sintering process, analysis, characterization

ZIF-4 powder was synthesised via a solvothermal route. For one batch, of 160 ml of dimethylformamide (DMF), 2.4 g zinc nitrate hexahydrate ($Zn(NO_3)_2 \cdot 6H_2O$), and 1.8 g of imidazole (Im) was mixed and filled in a glass jar with temperature resistant screw lid. The solution was held at 140 °C for 96 h. Precipitate ZIF-4 crystals were filtrated from the liqud. For solvent exchange, fresh ZIF-4-DMF was immersed in dichloromethane (DCM) during 48 h, while being stirred gently. The DCM was replaced after 24 h with fresh DCM. Solvent exchanged ZIF-4-DCM was desolvated at 140 °C during 48 h under vacuum (approximately 0.1 mbar). Complete desolvation was confirmed by Raman spectroscopy. Particle size distribution of the obtained pure ZIF-4 powder was measured using a Beckman Coulter LS 13 320 laser diffraction particle size analyser in suspension mode (S2).

The sintering process was performed under vacuum on a HP-D 10 SPS facility, FCT System GmbH, Germany. Powder sample were weighted (~2 g) and filled into the graphite dies. A type-K thermocouple was inserted centrally in a hole in the wall of the die. The process chamber was evacuated. The temperature was raised at a rate of 50 °C/min by resistive heat generated from passing a pulsed direct current (max. 0.35 kA, 4.65 V) through the graphite parts. After 2 minutes dwelling time, the samples cooled at approximately -50 °C/min. Detailed sintering log files of temperature, pressure, and compaction can be found in S5.

Fragments of the bulk samples were embedded in epoxy resin. The surfaces were polished with 0.25 μm water-based diamond suspensions and carbon coated. Back-scattered electron images were acquired on a FEI Qemscan Quanta650F operated at 10 kV, at a working distance of 13 mm.

Room-temperature powder X-ray diffraction (PXRD) data ($2\theta = 5-30°$) were collected with a Bruker-AXS D8 diffractometer using Cu Kα ($\lambda = 1.540598$ Å) radiation and a LynxEye position-sensitive detector in Bragg−Brentano geometry on a crushed portion of the sintered material. Temperature dependent powder diffraction data was collected on the same machine equipped with a MRI radiation-heating stage in air. Pure silicon powder was mixed with ZIF-4 and used as an internal standard for sample height displacement corrections. Rietveld fitting of diffraction patterns based on a ZIF-4 structure model from literature was performed using TOPAS (V6). Variable-temperature powder XRD data sets were fitted parametrically. First, only the silicon peaks were fitted, refining individual sample displacements with fixed *T*-dependent standard lattice parameters. Subsequently, ZIF-4 and ZIF*zni* were fitted with fixed specimen displacements based on published structural models[1,2].

Skeletal densities were measured by He-pycnometry using a Micromeritics Accupyc 1340. The typical mass used was 0.3 g. The values quoted (Table 1) are the mean and standard deviation from a cycle of 10 measurements. The bulk density of the macro-porous sample C was determined from its bulk volume and weight.

Thermomechanical analysis was performed using TMA Q400 system of TA instruments at heating rate of 5°C/min under 0.05 N static force in the temperature range from 20 °C to 550 °C.

Nanoindentation experiments were performed on an MTS Nanoindenter using a Berkovich diamond tip of 100 nm radius. Compression tests were carried out on a Tinius Olsen H5KS Benchtop Tester.

X-ray micro-tomography images were acquired on a Bruker Skyscan 1272 Micro-CT system. The resulting projections were processed into 3D data sets using a full cone beam Feldkamp reconstruction algorithm with NRecon software (Bruker).

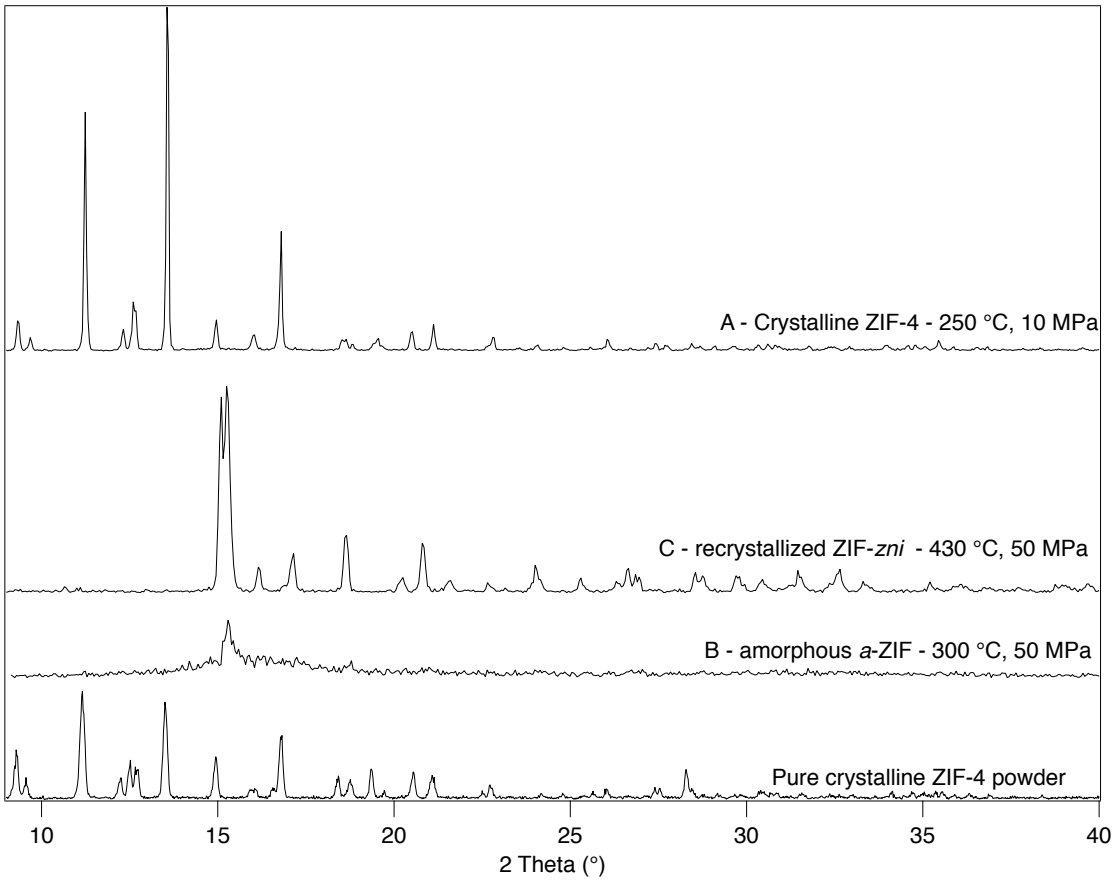

Figure S1. Powder X-ray diffraction patterns from crushed portions of sintered monoliths for phase identification and pure ZIF-4 powder.

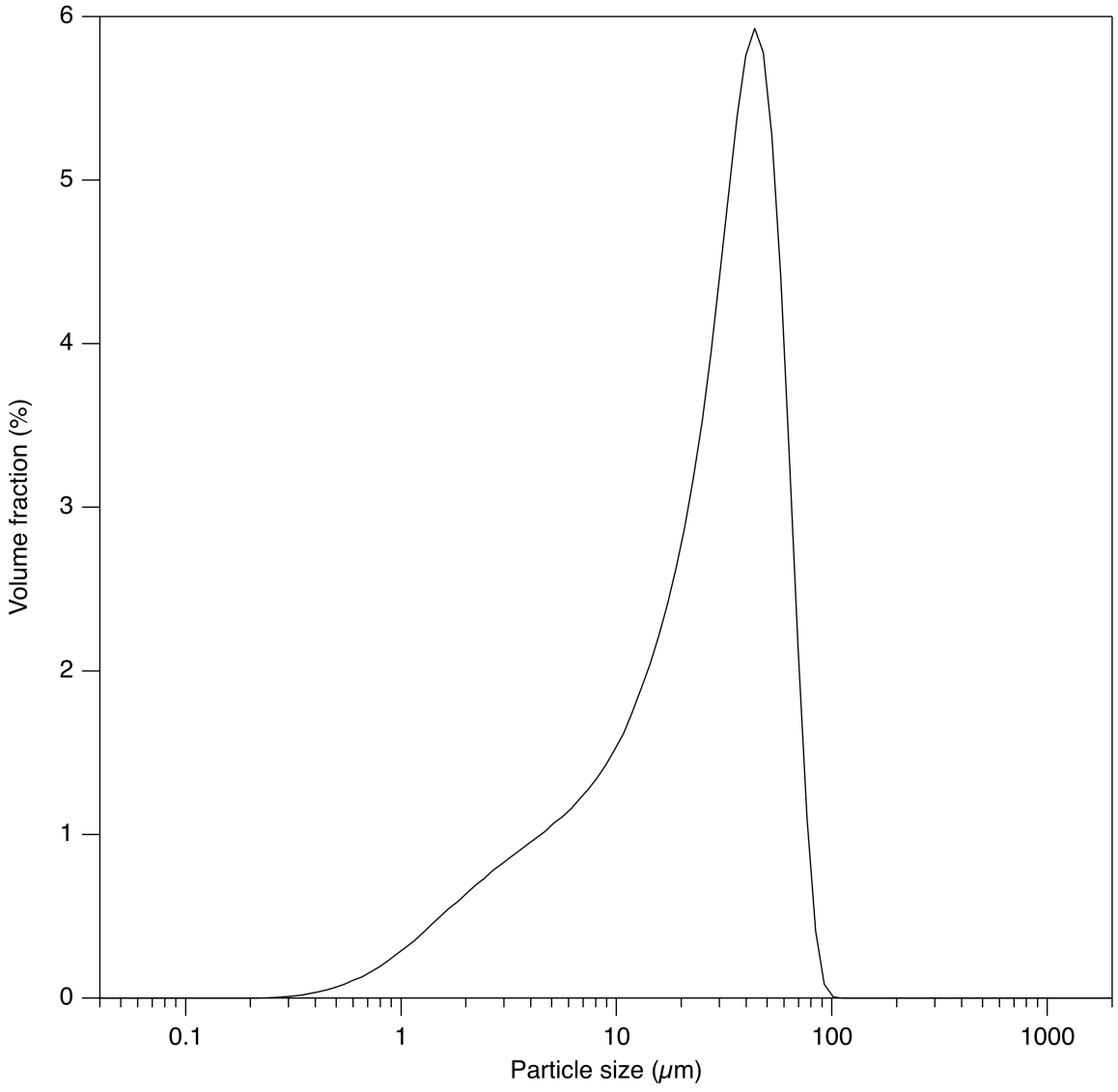

Figure S2. Particle size distribution of starting powder measured by Laser diffraction.

Sample B – amorphous a-ZIF-4

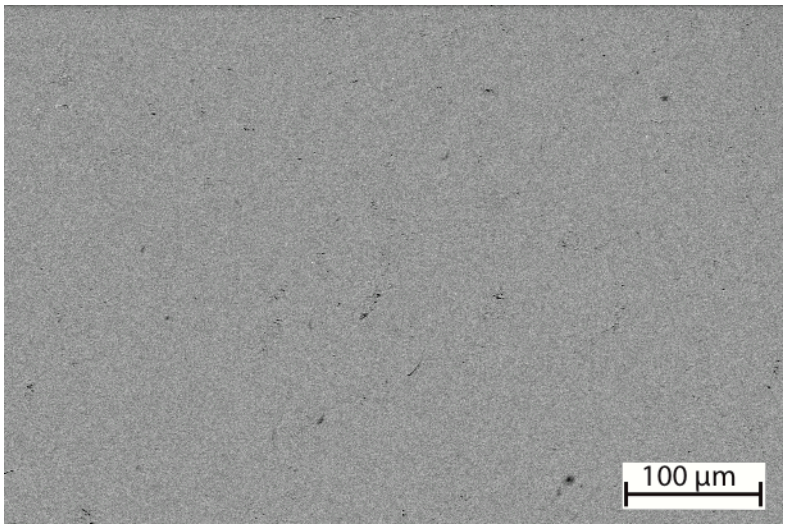

Sample C – recrystallized ZIF-zni

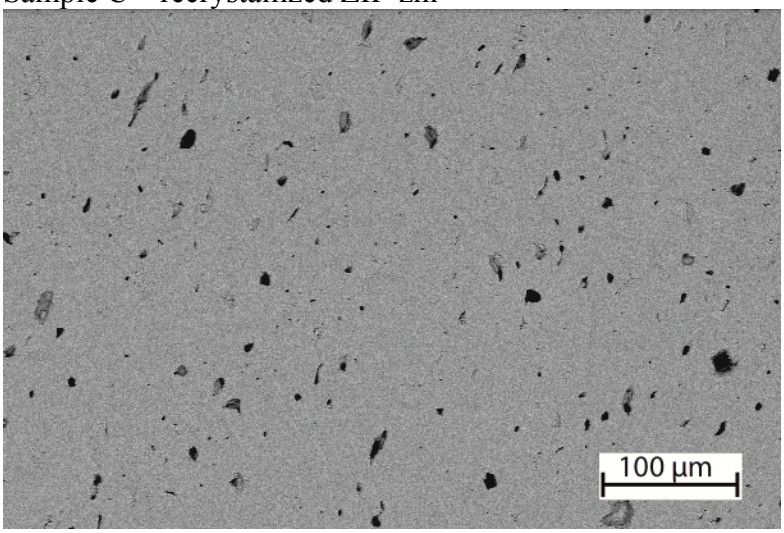

Figure S3. SEM images of Samples B and C. Backscattered electron images were recorded on polished surfaces. **Sample B:** Collapse of the crystallinity and softening of the grains supporting the originally highly porous microstructure lead to an almost fully densified microstructure. **Sample C:** recrystallization to ZIF-*zni* from amorphous *a*-ZIF entails a density increase, i.e. volume decrease, that could be responsible for the formation of isolated porosity (black spots).

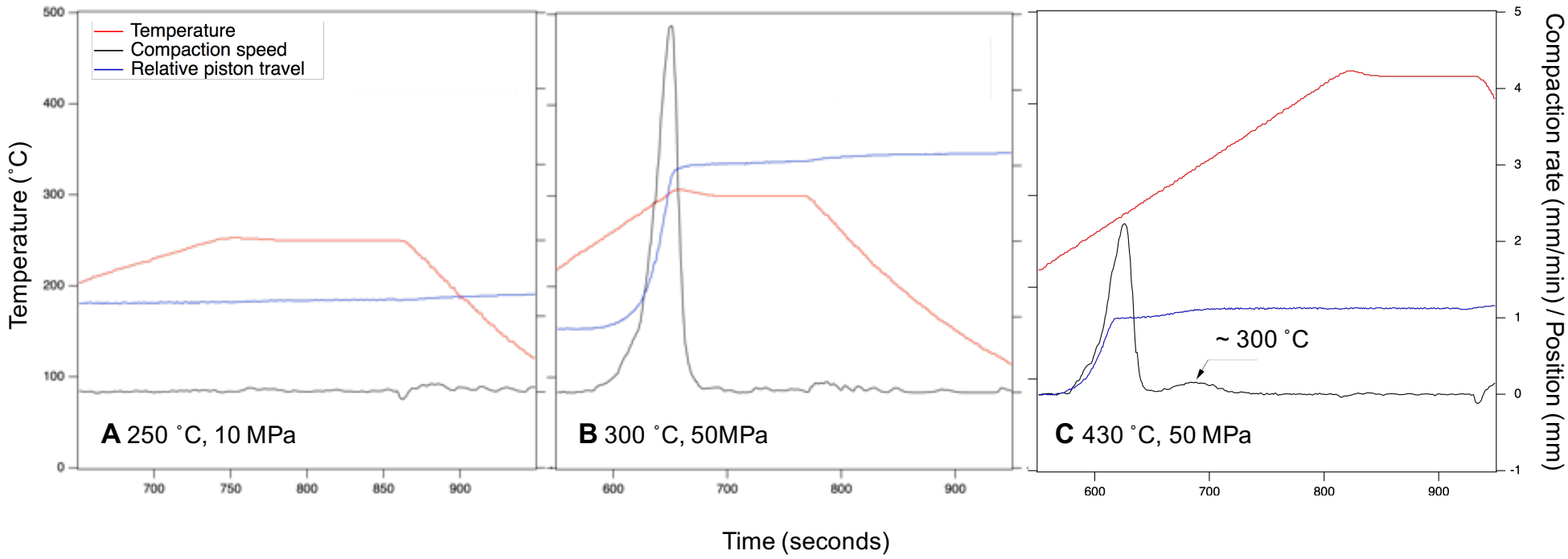

Figure S4. Sintering log data from individual runs. (A) Target temperature 250 ˚C and pressure 10 MPa, (B) target temperature 300 ˚C and pressure 50 MPa, (C) target temperature 430 ˚C and pressure 50 MPa.

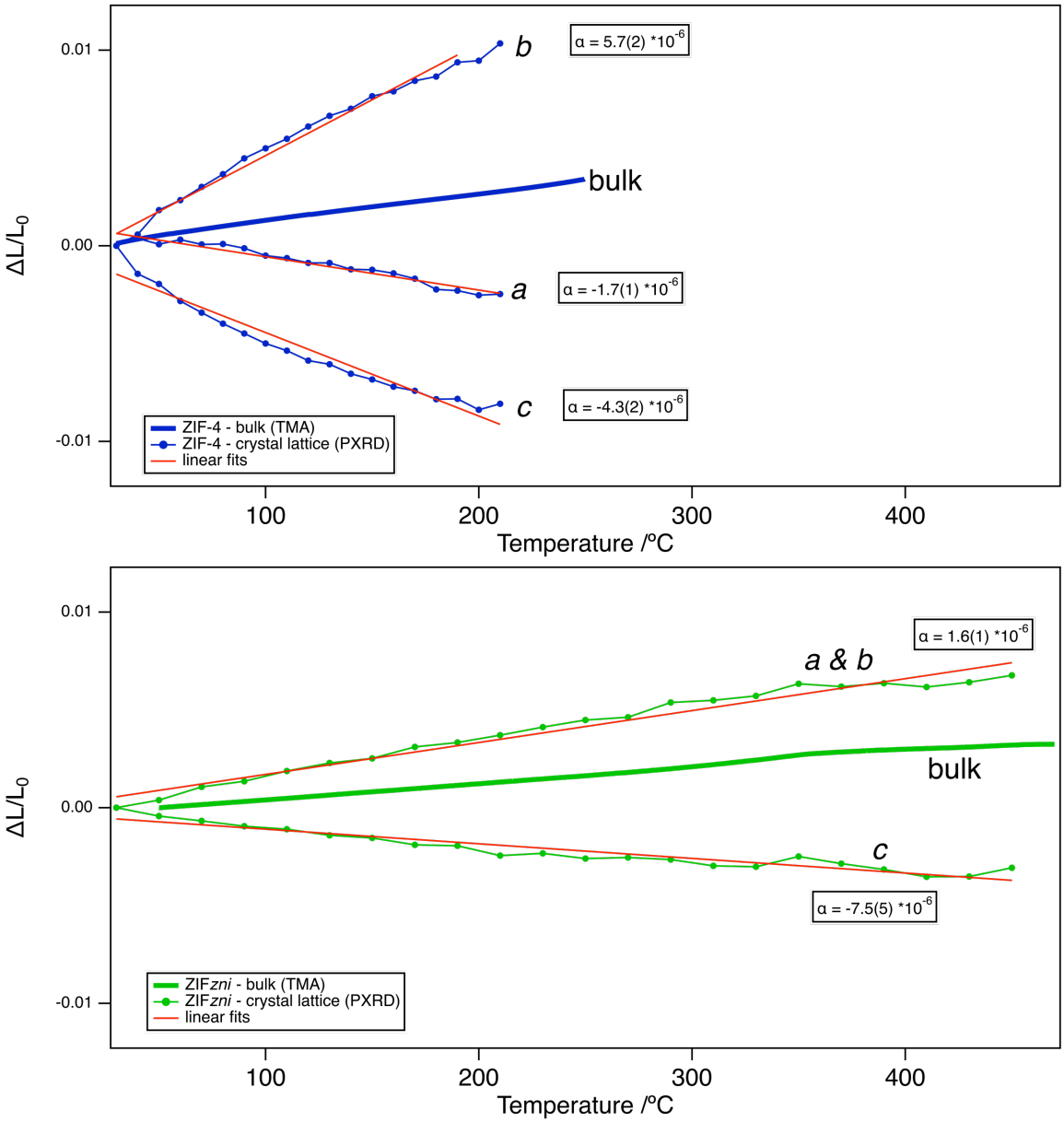

Figure S5. Temperature dependent relative unit cell dimensions of ZIF-4 (top) and ZIF-*zni* (bottom). ZIF-*zni* was prepared by heating ZIF-4 to 400 °C under vacuum (heating rate 0.5 °C/min). Thermal expansion coefficients α derived from the slope of the linear fits (red lines).

Supporting references

1 Lehnert, R.; Seel, F. Darstellung und Kristallstruktur des Mangan(II)- und Zink(II)-Derivates des Imidazols. *Zeitschrift für anorganische und allgemeine Chemie,* 1980, **464**, 187-194. doi:10.1002/zaac.19804640117

2 Park, K. S.; Ni, Z.; Côté, A. P.; Choi,J. Y.; Huang, R.; Uribe-Romo, F. J. ; Chae, H. K.; O'Keeffe, M.; Yaghi, O. M. Exceptional chemical and thermal stability of zeolitic imidazolate frameworks. *Proceedings of the National Academy of Sciences,* 2006, **103**, 10186-10191. doi:10.1073/pnas.0602439103